Article:
Pickering, Matthew David, Ghislandi, Sabina, Usai, Maria Raimonda et al. (2018) Signatures of degraded body tissues and environmental conditions in grave soils from a Roman and an Anglo-Scandinavian age burial from Hungate, York. Journal of archaeological science. pp. 87-98. ISSN: 0305-4403

https://doi.org/10.1016/j.jas.2018.08.007

Signatures of degraded body tissues and environmental conditions in grave soils from a Roman and an Anglo-Scandinavian age burial from Hungate, York

Matthew D. Pickering[a], Sabina Ghislandi[b], Maria Raimonda Usai[b,c†], Clare Wilson[d], Peter Connelley[e], Don R. Brothwell[b†] and Brendan J. Keely[a]*

[a] Department of Chemistry, University of York, Heslington, York, YO10 5DD, UK

[b] Department of Archaeology, University of York, The King's Manor, York, YO1 7EP, UK

[c]Dipartimento di Architettura e Design, Wilson, Piazza Pau Salit, Alghero, Italy

[d]School of Biological and Environmental Science, University of Stirling, Stirling. FK9 4LA, UK

[e]York Archaeological Trust, 47 Aldwark, York YO1 7BX, UK

ORCHID ID

Keely: 0000-0002-8560-1862

Pickering: 0000-0002-6234-2108

Wilson: 0000-0002-0287-8576

Highlights

- Signatures of degraded body tissues, gut contents and microbial activity from grave soils.
- Spatial variation in signatures with anatomical location and features of burial environment.
- *n*-Alkanals reveal highly localised regions of anoxia.
- Grave chemistry and preservation of the skeletal remains has been impacted by an adjacent cess pit.
- Pedogenic spherulites record broad changes in redox conditions within the Roman grave.

Keywords: Human burials; scientific archaeology; triacylglycerols; *n*-alkanals; bone cholesterol; redox conditions; Roman; Anglo-Scandinavian.

† Deceased on 26 September 2016 (DRB) and 13 May 2018 (MRU).

Abstract

Despite the importance of human burials in archaeological investigations of past peoples and their lives, the soil matrix that accommodates the remains is rarely considered, attention being focused mainly on visible features. The decomposition of a buried corpse and associated organic matter influences both the organic composition and, directly or indirectly, the microstructure of the burial matrix, producing signatures that could be preserved over archaeological timescales. If preserved, such signatures have potential to reveal aspects of the individual's lifestyle and cultural practices as well as providing insights into taphonomic processes. Using organic chemical analysis and soil micromorphology we have identified organic signatures and physical characteristics relating to the presence of the body, and its decomposition in grave soils associated with two human skeletons (one Roman age and one Anglo-Scandinavian age) from Hungate, York, UK. The organic signatures, including contributions from body tissues, gut contents, bone degradation and input from microbiota, exhibit spatial variations with respect to anatomical location and features of the immediate burial environment. In the Roman grave broad changes in redox conditions associated with the decomposition of the corpse and disturbance from the excavation and use of an Anglo-Scandinavian age cess pit that partially cuts the grave were evident. Leachate from the cess pit was shown to exacerbate the degradation of the skeletal remains in the regions closest to it, also degrading and depleting spherulites in the soil, through decalcification of the bone and liberation of bone-derived cholesterol into the soil matrix. The findings from this work have implications for future archaeo- and contemporary forensic investigations of buried human remains.

1 Introduction

The study of human burials in the archaeological record provides a unique glimpse into the lives (and deaths) of our ancestors. Investigations typically focus on the recording, recovery and analysis of the visible human remains, grave goods and burial structures (Brothwell, 1981). Although some well-preserved burials have provided evidence of clothing (Barfield, 1994; Hadian et al., 2012), organic grave goods (Barfield, 1994) and body tissues (O'Connor et al., 2011; Stead et al., 1986), the survival of perishable materials in a condition that can be visually recognised is rare and generally limited to particular burial environments (e.g. waterlogged, arid, frozen) and modes of preparation of the corpse (e.g. embalming and mummification). While organic materials were undoubtedly significant, widespread and varied components of human burials, in the vast majority of burials the extent of decay is such that evidence of these components is invisible to traditional archaeological techniques.

Organic chemical analysis is now an established tool in the field of archaeology and has been applied to many different types of archaeological remains (Evershed, 2008), including human remains. Bone

collagen can survive over archaeological timescales and is routinely isolated for stable isotope and radiocarbon analysis. Exceptional examples of soft tissue preservation have provided rare opportunities to study their protein and lipid compositions and thereby the extent and mechanisms of preservation (Evershed and Connolly, 1988; Gulaçar et al., 1990; Mayer et al., 1997; O'Connor et al., 2011). Likewise, chemical characterisation of organic residues associated with the wrappings of Egyptian mummies has provided information on the preparations used by ancient embalmers (Buckley and Evershed, 2001). By contrast, the potential for the soil in contact with buried human remains to retain molecular information relating to decayed organic components of the burials has received little attention. Such organic remains could relate to components from the body tissues of the interred, from the stomach and gut contents, from formulations used in preparing the body for burial and from substances associated with grave goods and burial structures, such as a coffin. Each of these sources has potential to inform the archaeological interpretation: components established to derive from the body tissues, whether or not the physical remains survive, could provide opportunities for isotopic analysis and hence consideration of differences in diet among past populations (Stott et al., 1999); stomach contents can reveal information regarding the balance of plant vs meat in the meals immediately prior to death (Pickering et al., 2014); formulations used in burial rituals could reveal commonalities and differences among individuals within localities and over time; signatures from grave goods could reveal the nature of now decayed materials that were placed within the graves and signatures of the burial structures (Burns et al., 2017) could also reveal commonalities and differences over time and with geographical location. In order for organic signatures to be meaningfully employed it is necessary to gain insights into the nature and extent of their alteration in the environments particular to graves. Whilst much variation can be expected according to burial practice, soil composition and chemistry, hydrology and age of burial, some generalities can be anticipated owing to the presence of a substantial amount of organic matter in a somewhat defined space.

Grave soils from contemporary human burials have been shown to contain chemical signatures of degraded adipose tissue (Bull et al., 2009; Forbes et al., 2002). Given that the recalcitrance of lipids allows their survival over geological timescales (Eigenbrode et al., 2008), informative chemical signatures from wide variety of sources have the potential to be preserved in archaeological grave soils. We present results of the chemical and micromorphological analysis of grave soils and sediments from two human burials from Hungate, York (UK), one of Roman age and the other of Anglo-Scandinavian age.

2 Experimental

2.1 Excavation

The Roman age grave (C51364, 1st – 4th C AD) and Anglo-Scandinavian age grave (C53700, ^{14}C date AD 870 - 980) were sampled for the InterArChive project in 2010 and 2011 during excavation of the Hungate site. Both were undisturbed burials, containing articulated skeletons (Fig. 1). The graves presented differences in the levels of preservation, both in terms of completeness of the skeletal remains and in the physical condition of the bones. Whereas the bone in the Anglo-Scandinavian burial was very well preserved, that in the Roman burial had lost much structural integrity and was incomplete, particularly the upper left side of the remains (Fig. 1).

Figure 1. Left panel C53700: Anglo-Scandinavian age burial (AD 870-980) containing the skeletal remains of an adult. During excavation, degraded wood was identified believed to have once been a wooden lid covering the remains. Right panel C51364: poorly preserved skeletal remains of an adult (Roman age ~ 3rd century AD) and a nearby Anglo-Scandinavian age cess pit (Context 2652) that cuts the grave.

2.2 Sampling

Controls were collected from non-grave soil from the site (C1) and from grave fill above the level of the skeletal remains, C2 and C3, as essential comparators of grave fill that has not been in contact with the buried remains (Fig. 2).

Samples of the burial matrix were collected in line with the InterArChive sampling strategy (Usai et al., 2014) from key anatomical locations on the skeleton (Table 1). The maximum number of prescribed points around the skeletal remains were targeted for chemical analysis and 4 key areas; head (1), pelvis (2) and feet (3/4) were targeted for micromorphological analysis (Table 1). Additional samples (prefixed by the letter 'A') were collected in response to specific features of the individual graves and from a cess pit adjacent to the Roman burial. Samples for micromorphology were collected from undisturbed archaeological sediment or grave fills using Kubiena tins (83 × 50 × 32 mm, 83 × 55 × 42 mm, and 65 × 38 × 28 mm). On return to the laboratory, samples were refrigerated prior to thin section preparation. Samples for chemical analysis were collected proximal to the skeletal remains or feature using a spatula, wrapped in pre-cleaned foil, placed in geochemical sample bags and stored cold. On return to the laboratory, samples were stored frozen until required for analysis.

2.3 Manufacture of thin sections

The samples were dried in the tins through acetone vapour exchange (Miedema et al., 1974) and impregnated under vacuum with a slow curing polyester resin (Polylite 32320-00). The resulting consolidated soil blocks were cut to produce the thin sections. The cut sections were back-polished, mounted, cut and ground to 30 μm thickness, with final 3 μm and 1 μm polishes.

2.4 Optical microscopy

Micromorphological observations were performed using a petrographic microscope (Zeiss AxioLab A1) equipped with a Zeiss AxioCamERc5s camera and AxioVision imaging software. The standard terminologies proposed by Bullock et al. and by Stoops (Bullock et al., 1985; Stoops, 2003) were adopted for the descriptions of the slides and semi-quantitative estimation of the features.

2.5 Scanning electron microscopy-energy dispersive X-ray analysis (SEM-EDS)

SEM-EDS analyses were conducted at the University of Stirling employing an EVO MA 15 Zeiss scanning electron microscope with workflow automation and an Oxford Instruments INCA X-Max EDS to provide micro-chemical data of fine material and inorganic pedofeatures of uncertain interpretation (Courty et al., 1989; Fitzpatrick, 1993; Goldberg and Macphail, 2003). Standard operating conditions were 8.5 mm working distance and 20 kV accelerating voltage. Calibration was achieved through the analysis of standard cobalt every 2 h and standard dolomite at the beginning of each session. A minimum of seven individual point analyses were carried out for each measured region. The measurements of O and C were excluded owing to the presence of the resin in which the samples were consolidated and weight percent data were normalized to 100%.

Table 1. Soil samples collected for the two graves from Hungate, York, UK.

Anglo-Scandinavian burial C53700			Roman burial C51364		
Sample Number[†]		Position	Sample Number[†]		Position
C1		Control (non-grave soil)	C2	M	Control (upper grave fill)
C2		Control (lower grave fill)	C3	M	Control (lower grave fill level with top of skull)
C3		Control (lower grave fill)	1	M	Skull
1	M	Skull	2	M	Sacrum
1b		Below skull	3		Left foot
2	M	Sacrum	4		Right foot
2b		Below sacrum	3 & 4	M	Between feet
3		Both feet	5		Left shoulder
5		Below left shoulder	6		Right shoulder
6		Below right shoulder	7		Left elbow
7		Below left elbow	8		Right elbow
8		Below right elbow	9		Left hip
9		Below left hip	10		Right hip
10		Below right hip	11		Left knee
11		Below left knee	12		Right knee
12		Below right knee	13		Left iliac
13		Below left iliac	14		Right iliac
14		Below right iliac	15		Sternum
15		Below sternum	16		Right hand
A1		Right scapula	A1		Wall of cess pit (context 2652)
A2		Dark soil right pelvis	A2		Material excavated from cess pit (context 2652)
A3		Coccyx	A3		Intracranial sediment
			A4		Abdominal region
			A5		Dark soil within pelvis

[†] Sample number corresponds to the standard sampling locations defined in Usai et al., (2014). Unless specified otherwise the soil adjacent to the bone was collected. Samples prefixed by the letter A represent samples additional to the standard sampling locations. M indicates that an undisturbed block sample for micromorphological analysis was collected in addition to a loose soil sample.

2.6 Preparation of materials and extracts for chemical analysis

All solvents used were analytical grade or higher. All glassware was baked (450°C, 6 h) prior to use using a Pyroclean Trace oven (Barnstead International, USA) to remove organic contaminants. Frozen soil samples were freeze dried using a HETO PowerDry PL3000 (Thermo, Hemel Hempstead, UK). Dry soils were disaggregated with a pestle and mortar, and sieved using 1 mm, 400 µm and 200 µm sieves. All subsequent work was performed on the sub 200 µm fraction. Extraction was performed using an accelerated solvent extraction system (ASE 350, Dionex, Hemel Hempstead, UK). Prior to loading soil samples, the empty extraction cells were subjected to extraction using the same solvents and conditions as for the samples. Soil (3-6 g) was loaded into 5 ml stainless steel cells and extracted three

times with dichloromethane:methanol (9:1 v/v; 5 min at 100°C and 1500 psi). A blank extraction was also performed to assess whether any contamination was being introduced at the extraction step. Solvent was removed using a rotary vacuum concentrator (RVC 2-25, Christ, Osterode am Harz, DE). The total extract was divided into two portions, one of which was fractionated using a custom-made glass chromatography column (90 mm x 10 mm i.d.) packed with silica gel (750 mg, height in column = 20 mm). The column was conditioned by washing with three bed volumes each of dichloromethane:methanol (1:1, v/v) and dichloromethane followed by equilibration with hexane. The extract to be fractionated was dissolved in dichoromethane (200 µl), spiked onto silica gel (40 mg) and the solvent removed in vacuo. The impregnated silica was loaded onto the top of the packed chromatography column. The column was washed with three bed volumes each of i) hexane, ii) hexane:toluene (1:1, v/v), iii) hexane:ethyl acetate (4:1, v/v) and iv) dichloromethane:methanol (1:1, v/v) to generate four chromatographic fractions: i) aliphatic hydrocarbons, ii) aromatic hydrocarbons and *n*-alkanals, iii) alcohols and esters and iv) acids, respectively. Solvent was removed using a rotary vacuum concentrator.

2.7 Derivatisation

Total extracts and polar (iii and iv) fractions were reconstituted in dichloromethane:methanol (2:1, v/v; 300 µl) followed by addition of trimethylsilyl diazomethane (20 µl) and allowed to react for 30 min, before drying under a gentle stream of nitrogen gas. Immediately prior to analysis, total extracts and polar fractions were heated with *N,O*-bis(trimethylsilyl)trifluoroacetamide (100 µl, containing 1% trimethylchlorosilane) and 5 drops of pyridine for 1.5 h at 60°C before removing excess derivatising agent under a gentle stream of nitrogen gas.

2.8 Total organic carbon (TOC) analysis

Total organic carbon (TOC) analysis was performed using a Flash 2000 elemental analyser (Thermo, Hemel Hempstead, UK) fitted with a MAS200R autosampler, chromatographic column and thermal conductivity detector. Helium was used as a carrier gas at a flow rate of 140 ml min^{-1}. Soil samples (10-15 mg) were weighed using a XS3DU microbalance (Mettler Toledo, Leicester, UK) into silver foil capsules. Samples were treated with 2 drops of hydrochloric acid (6 M) to destroy carbonates before heating to 80°C for 6 min to drive off excess acid solution. Foil capsules were folded to exclude air. Samples were combusted in a quartz reactor tube packed with copper oxide granules and electrolytic copper wires held at 900°C. Sample introduction coincided with a pulse of oxygen (250 ml min^{-1}, 5 s). Instrument control, data acquisition and processing was by Eager Xperience V1.11 (Thermo, Hemel Hempstead, UK).

182 *2.9 Gas chromatography (GC) and gas chromatography-mass spectrometry (GC-MS)*

183 Total lipid extracts were analysed using a Trace GC Ultra gas chromatograph (Thermo, Hemel
184 Hempstead, UK) equipped with a Triplus autosampler, a fused silica capillary column (J&W DB-5, 60
185 m x 0.32 mm i.d., 0.25 μm film thickness, Agilent, Wokingham, UK) and a flame ionisation detector
186 (FID). Samples were prepared in dichloromethane and volumes of 1 μl injected onto the column via
187 a split/splitless injection port operating in splitless mode (280°C, split flow 1:25, splitless time 0.8 min).
188 The oven temperature was programmed from an initial temperature of 70°C to 130°C at a rate of 20°C
189 min^{-1} and then to 320°C at a rate of 4°C min^{-1} where it was held for 40 min. Helium was used as a
190 carrier gas at a flow rate of 2 ml min^{-1}. The FID was held at 330°C. Instrument control, data acquisition
191 and analysis was by ChromQuest 5.0 V3.2.1 (Thermo, Hemel Hempstead, UK).

192 Chromatographic fractions (i-iv) were analysed using an identical gas chromatograph to that above
193 equipped with an ultrafast column module (UFC-5, 10 m x 0.1 mm i.d., 0.1 μm film thickness, Thermo,
194 Hemel Hempstead, UK). Samples were prepared in dichloromethane for analysis and volumes of 1 μl
195 injected onto the column via a split/splitless injection port operating in split mode (280°C, split flow
196 1:100) and the FID held at 330°C. The column oven was programmed from an initial temperature of
197 50°C (0.5 min isothermal) to 330°C at a rate of 90°C min^{-1} where it was held for 4 min. Helium was
198 used as the carrier gas at a flow rate of 0.5 ml min^{-1}.

199 GC-MS analysis was performed on selected fractions using a 7860A gas chromatograph (Agilent,
200 Wokingham, UK) equipped with a 7683B Series autosampler coupled to a GCT Premier Micromass
201 time of flight mass spectrometer (Waters, Elstree, UK). Separation was achieved on a fused silica
202 capillary column (Zebron, ZB-5, 30 m x 0.25 mm i.d., 0.25 μm film thickness, Phenomenex,
203 Macclesfield, UK). Samples were prepared in dichloromethane for analysis and volumes of 1 μl
204 injected onto the column via a split/splitless injection port operating in split mode (280°C, split flow
205 1:5). The oven was programmed from an initial temperature of 70°C to 130°C at a rate of 20°C min^{-1}
206 and then to 320°C at a rate of 4°C min^{-1} where it was held for 40 min. Helium was used as the carrier
207 gas at a flow of 1 ml min^{-1} and the MS transfer line set to 300°C. Mass spectra were acquired over the
208 range *m/z* 50-750 (cycle time 0.2 s) using an electron ionisation energy of 70 eV. Instrument control,
209 data acquisition and processing was by MassLynx V4.1 (Waters, Elstree, UK). Compounds were
210 identified from interpretation of their mass spectra and comparison with library spectra (NIST 08)
211 where available.

212 *2.10 High performance liquid chromatography-multistage tandem mass spectrometry (HPLC-MS^n)*

213 HPLC-MS^n analysis of triacylglycerols was performed on selected total extracts according to Method J
214 of (Hasan, 2010) using a Dionex Ultimate 3000 rapid separation liquid chromatograph, controlled by

Chromeleon 6.8 (Dionex, Hemel Hempstead, UK), coupled to a HCTultra ETD II quadrupole ion trap mass spectrometer (Bruker Daltonics; Coventry, UK) fitted with an atmospheric chemical ionisation (APCI) source. Briefly, samples were prepared in hexane:propan-2-ol:acetonitrile (1:1:1, v/v/v). Lipid separation was accomplished using two 3 µm Spherisorb ODS2 columns (150 x 4.6 mm i.d.) coupled in series, using a ternary solvent gradient system comprising acetonitrile, dichloromethane and ammonium acetate in methanol (0.01 M) at a flow rate of 1 ml min^{-1}. APCI was operated in positive ion mode using the following settings: vaporiser temperature 450°C, nebuliser gas (N_2) 50 psi, drying gas (N_2) flow rate 3 L min^{-1}, drying gas temperature 150°C, corona 4000 nA and capillary voltage -4000 V. Mass spectra were acquired in Ultra Scan mode over the range *m/z* 300-950 with a cycle time of 0.025 s. Online multistage tandem mass spectra (to MS^3) were generated following selection of the most abundant ion in the mass spectrum for collision induced dissociation. The isolation width was set to 4 *m/z* units, maximum accumulation time was fixed at 200 ms and Smart Fragmentation set to between 30-200% of a fragmentation amplitude of 1.0 V. MS control, data acquisition and processing was by Compass EsquireControl 6.2 and Compass DataAnalysis 4.0 (Bruker Daltonics; Coventry, UK).

3 Results and Discussion

Chemical and micromorphological analyses of samples of burial soil, collected from numerous specific locations (e.g. Fig. 2; full sample list in Table 1) around the skeletal remains of the Roman and Anglo-Scandinavian burials, were compared with controls to identify features and signatures uniquely associated with the burials. The soil particles were dominated by coarse grains of quartz with clays dominating the fine material (Table 2). The soil in the Roman burial was apedal whereas that in the Anglo-Scandinavian burial contained weakly developed granular peds and more voids. Given their different positions within the stratigraphic profile it is not possible to determine if the difference between the two graves relates to intrinsic differences during soil formation or to post depositional disaggregation of peds in the Roman grave. The sediment from both graves contained fragments of humified plant matter including gymnosperm wood in the Anglo-Scandinavian grave. Fungal hyphae were also identified in the Anglo-Scandinavian grave in the area of the pelvis and sclerotia in the areas of the skull and pelvis. The dominant pedofeatures in the Roman grave were spherulites, goethite crystals, Fe/Mn nodules and clay coatings indicating variations in redox conditions and water saturation. Amorphous phosphate was absent or very low around the torso in the Roman grave and the concentrations at the feet and in the controls were anomalously low compared with most other graves examined in Hungate (Ghislandi, 2016). The Anglo-Scandinavian grave contained higher levels of amorphous phosphate throughout the thin sections and vivianite in association with the bone. Hence, parts of the Roman grave may have been subjected to processes that caused leaching of

phosphorus. The presence of Fe/Mn nodules in the Anglo-Scandinavian grave indicate changes in water saturation, though in a generally more oxidising environment than in the Roman grave.

The organic extracts of the soils were analysed by gas chromatography-mass spectrometry (GC-MS) and high performance liquid chromatography-multistage tandem mass spectrometry (HPLC-MS^n) to determine the distributions of lipid components in the soils. The extracts of all samples and controls from both graves were dominated by autochthonous components of soil organic matter, mainly homologous series of *n*-alkanoic acids (C_{16}-C_{34}), *n*-alkanols (C_{18}-C_{34}) and *n*-alkanes (C_{20}-C_{35}), the distributions being characteristic of the leaf waxes of vascular plants (Eglinton and Hamilton, 1967). In addition, phytosterols 24-ethylcholest-5-en-3β-ol (sitosterol), 24-ethylcholest-5,22-dien-3β-ol (stigmasterol) and 24-methylcholest-5-en-3β-ol (campesterol) were detected.

Despite the strong overprint from the natural soil organic matter, the samples associated with the skeletal remains exhibited distinct differences to the controls, generally exhibiting elevated levels of triacylglycerols (TAGs) (e.g. Figs. 2a and 3); di-$C_{16:0}$ and $C_{16:0}$/$C_{18:0}$ 1,2- and 1,3-diacylglycerols (DAGs); $C_{16:0}$ and $C_{18:0}$ monoacylglycerols (MAGs); $C_{16:0}$ and $C_{18:0}$ fatty acids (Fig. 2b); $C_{16:0}$ and $C_{18:0}$ *n*-alkan-1-als (Fig. 2b) and branched chain *iso* (*i*-) and *anteiso* (*ai*-) $C_{15:0}$ and $C_{17:0}$ fatty acids (Fig. 2c). The TAG concentrations associated with the Anglo-Scandinavian remains were around an order of magnitude greater than those for the Roman remains. Though TAGs have been identified from within the protective environment of archaeological ceramics (Garnier et al., 2009; Kimpe et al., 2001; Mirabaud et al., 2007; Šoberl et al., 2008) their occurrence in grave soils has not been reported previously. The elevated levels of the TAGs, the primary constituents of animal fats and vegetable oils, associated with the skeletal remains suggests they derive from adipose tissue. The low levels associated with the controls (*e.g.* Fig. 2) may reflect minor contributions from plant sources or background levels from previous burials within the cemetery. Notably, the TAG distributions in the soil samples are dominated by saturated components (Fig. 3b) whereas fresh human adipose tissue comprises predominantly (99%) unsaturated TAGs (Mayer et al., 1997). Generally, unsaturated components are more susceptible to degradation (e.g. via oxidative cleavage) than their saturated counterparts. In addition, human lipases have been shown to exhibit a preference for acyl moieties at the *sn*-1 and *sn*-3 positions on the glycerol backbone as well as for unsaturated moieties (Jensen et al., 1994; Raclot and Groscolas, 1993). Preferential degradation of TAGs containing unsaturated acyl chains could explain the observed predominance of saturated TAGs in the soil extracts. Comparison of the acyl chain distributions of the saturated TAGs in the soil extracts from around the skeletal remains (Fig. 3c) with the saturated TAG-derived fatty acid distributions of fresh human adipose tissue (Hodson et al., 2008) reveals a strong similarity (A; Fig. 3c). By contrast, complete reduction of monounsaturated and of all unsaturated fatty acids of human adipose TAGs would generate the predicted ratios shown for B and

C (Fig. 3c), respectively. Thus, extensive post-depositional alteration of the body fats is evident and involves preferential loss of unsaturated TAG moieties. The TAG distributions in the soils around the skeletal remains (Fig. 3b) exhibit a striking similarity to those reported for the adipocere of a 65 year old ice mummy and the skin of a 5300 year old ice mummy (Mayer et al., 1997), supporting the genesis of these signatures from human adipose tissue. In those cases, preservation of TAGs may be attributed largely to the physiochemical barriers to degradation: encasement in ice and desiccation, respectively. A study involving augmentation of three different soils with a model saturated TAG (tristearin) showed that release of fatty acids within the first weeks of incubation at 20°C could be attributed to the soil microbial community (Hita et al., 1996). It is remarkable, therefore, that TAG signatures of adipose tissue can be recovered from grave soils after more than 1600 years since interment. TAGs and cell membrane phospholipids are degraded in soils by stepwise hydrolysis to fatty acids and glycerol (and phosphate in the case of phospholipids), which explains the elevated levels of DAGs, MAGs and $C_{16:0}$ and $C_{18:0}$ fatty acids compared with the controls (e.g. Fig. 2b).

The $C_{16:0}$ and $C_{18:0}$ *n*-alkan-1-als associated with the skeletal remains have not been reported as significant components of soils and were not detected in the controls (Fig. 2b). Short chain *n*-alkan-1-als, principally C_{16} and C_{18} components, occur as both free and plasmalogen-bound components in various animal tissues (Gilbertson et al., 1967; Rapport and Lerner, 1959; Wittenberg et al., 1956) although their amounts are too low (relative to other lipid classes such as fatty acids) to represent a significant source of *n*-alkan-1-als in the soil extracts, where they represent approximately 10% abundance relative to summed $C_{16:0}$ and $C_{18:0}$ fatty acids (Fig. 2b). The most likely source that would explain the concentrations of *n*-alkan-1-als in the soil extracts is reduction of fatty acids (e.g. mediated by anaerobic bacteria). The concentrations of *n*-alkan-1-als in the soils are not, however, controlled by fatty acid concentration alone: the differences in $C_{16:0}$ and $C_{18:0}$ fatty acids concentrations with anatomical location do not correlate with those of the corresponding *n*-alkan-1-als (Fig. 2b), most notably around the pelvis in the Anglo-Scandinavian grave. Features of bone morphology (for example the skull or sacrum) could restrict water movement and contribute to highly localised regions of anoxia that favour reduction of organic matter. Thus, the reductive transformation of fatty acids to *n*-alkan-1-als, and the survival of the relatively labile aldehyde species themselves, is strongly indicative of persistent oxygen-limited conditions within areas of the grave, with higher *n*-alkanal:fatty acid ratios reflecting localised regions of more extensive anoxia.

312 Table 2a. Micromorphological descriptions of the sediments from the Roman age grave (C51364) and Scandinavian age grave (C53700) from Hungate, York,
313 UK). PPL = plane polarised light, XPL = cross polarised light.

Burial	Microstructure	Voids	Mineral components	Organic components	Pedofeatures
C51364 (Roman)	Two principal c/f related distributions either strongly separated or intermingled: porphyric and poorly/moderately sorted (10-30% by area) or chitonic and moderately/well sorted (70-90% by area). Several intermediate distributions. Porphyric areas were brown/light brown/yellowish brown in PPL and brown/yellow or isotropic in XPL, with dotted limpidity and speckled b-fabric. Chitonic areas were yellowish or reddish brown in PPL and orange/yellow or isotropic in XPL, with speckled or parallel striated b-fabric. Samples were apedal.	Chambers, 500-2000 µm with undulating surfaces, in the areas of the feet (8%), skull and C3 (5%) and pelvis (2%). Channels at all positions (5% except for skull: 8%). Modified complex voids only in the areas of skull and pelvis (5%) and control C2 (8%). Frequency of packing voids increased from the skull to the control C2, absent from the pelvis. Planar voids, thickness 100-1500 µm, in areas of skull (15%), pelvis and feet (5%) and C3 (8%).	Mineral components mostly sub-angular and not weathered quartz (45-55%). Occasional fragments of quartzite in the areas of the feet (2%) and C2 (5%). Rare grains of biotite were in the area of the skull (2%).	Fragments of weathered or partially weathered humified plant structures in all samples (2%) except control C3. Plant remains, 50-2000 µm, brown/black in PPL and isotropic in XPL. Some coarser fragments exhibit vessels, hence angiosperm-derived.	Sideritic spherulites in the areas of skull, pelvis, feet and C3 exhibit morphological differences: Group 1 (skull 5-10%, 5-12 µm; feet 10-20%, 2-5 µm; pelvis 2-5%, 5-12 µm): orange in PPL; Maltese cross extinction in XPL. Infillings in pores and within fine material in the areas of skull and pelvis. Sealed between well-preserved layered coatings of Fe rich fine material in area of feet. Group 2 (C3, skull and pelvis): 5-20 µm; yellow in PPL, amorphous in XPL; infillings in pores and among mineral grains. Some have coalesced to form dumbbell structures. Group 3 (feet): 5-15 µm; orange/yellow in PPL. Some present two distinct layers with high contrast at junction; only outer layer exhibits Maltese cross extinction; core amorphous in XPL. Infillings of goethite in voids in area of skull (8%): loose discontinuous or dense incomplete. Occurs as fan-like crystals, orange/red colour in PPL and reddish brown or isotropic in XPL and with parallel striated b-fabric. Sub-angular/sub-rounded Fe/Mn nodules (50-500 µm, 5%) in all samples except control C2. Thin dark brown coating around voids, probably organic in origin, in areas of feet (8%), skull and pelvis (5%). External quasicoatings of clay around voids in area of pelvis (8%) and C2 (5%), clay textural impregnations in area of skull. Coatings of amorphous phosphate in control samples (5-10%).

314

315 Table 2b. Micromorphological descriptions of the sediments from the Roman age grave (C51364) and Scandinavian age grave (C53700) from Hungate, York,
316 UK).

Burial	Microstructure	Voids	Mineral components	Organic components	Pedofeatures
C53700 (Anglo-Scandinavian)	Two different fabrics: A (50-85%), B (20-50%) and C (10%) in varying proportions. Type A: close porphyric c/f related distribution, good sorting. Fine material, 10-40%, yellowish brown/brown in PPL and reddish brown or yellow/brown in XPL, with dotted limpidity and speckled b-fabric. Type B: open porphyric and well sorted. Fine material, 60-80%, reddish brown or yellowish brown in PPL and yellow/brown in XPL, dotted limpidity and speckled or parallel striated b-fabric. Type C (area of vertebrae): chitonic c/f related distribution, good sorting, yellow/orange in PPL, yellow or isotropic in XPL, limpid or dotted limpidity, parallel striated b-fabric. Samples from areas of skull and pelvis exhibit spongy appearing microstructures. Weakly developed granular peds (5-10%) in the area of vertebrae: fine in size and unaccommodated.	Chambers in areas of pelvis (8-15%) and skull (2%). Channels in areas of pelvis (8-15%) and vertebrae (10%). Modified complex voids in areas of skull (8-25%), vertebrae and pelvis (8%). Packing voids in the areas of the skull (8%), pelvis (5%) and vertebrae (15%).	Quartz dominant in all samples (30-50%), quartzite only in areas of pelvis (2%) and vertebrae (5%). Flint in area of pelvis (2%).	Amorphous organic matter in area of skull (2%). Humified plant structures (200-2000 µm) in all samples (2-5%). Occasional fragments characterized by vessels, hence angiosperm-derived. Gymnosperm wood indicated by single imprint of fragment in fine material in area of pelvis. Same sample exhibits humified plant (>2000 µm) comprising four fragments oriented parallel to the resting plane, circular/angular brown cells with infilling of fine material. Light brown in PPL and brown or isotropic in XPL. Fungal hyphae present in groundmass in area of pelvis. Sclerotia (20-200 µm) in areas of skull and pelvis (2%). Occasional roots in area of pelvis: orange in PPL and partially white in the internal section in XPL.	Amorphous phosphates in all samples, most frequent in area of pelvis (5-20%). Occur as coatings voids, nodules and strong impregnations in fine material; light yellow or yellow in PPL and isotropic in XPL; some exhibit crystallitic layers, occasionally weathered with granular aspect in pelvic area. Occasional amorphous phosphate coatings around spherical Mn nodules in areas of skull and pelvis. Single occurrence of vivianite (100-150 µm) in area of pelvis. Red redox impregnations in areas of pelvis and vertebrae (5%). Fe/Mn nodules in area of skull (2-8%) and occasional in the other samples. Clay coatings around mineral grains in areas of skull (2%) and pelvis (5%).

317

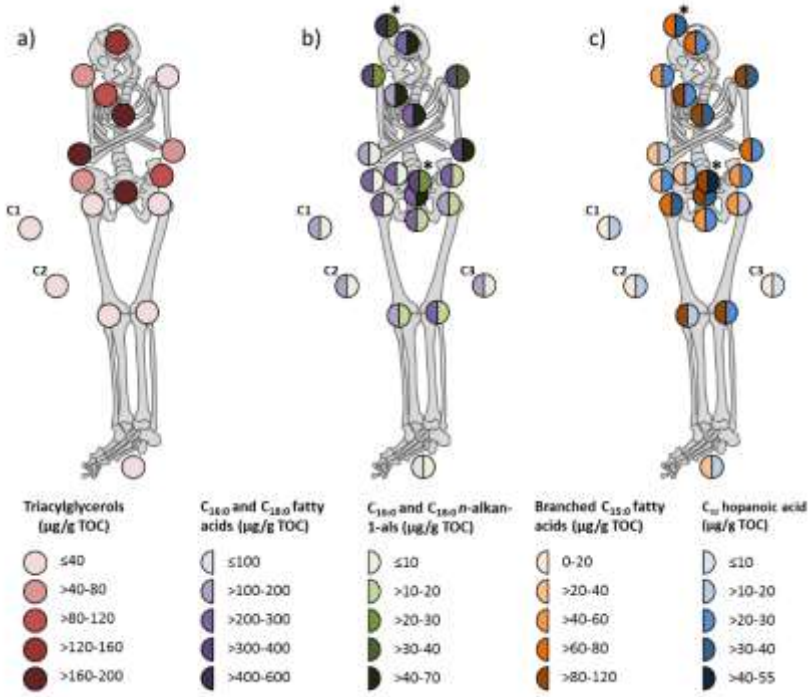

318

319 **Figure 2.** Variation in concentrations of specific lipids in the Anglo-Scandinavian age burial C53700: **a)**
320 combined triacylglycerols (TAGs; red shades), **b)** combined $C_{16:0}$ and $C_{18:0}$ fatty acids (purple shades)
321 combined $C_{16:0}$ and $C_{18:0}$ *n*-alkan-1-als (green shades) and **c)** combined *i*- and *ai*-$C_{15:0}$ fatty acids (orange
322 shades) and bishomohopanoic acid (C_{32}; blue shades). All soil samples were collected from below the
323 skeletal remains except for samples marked with an asterisk (*) which were collected from adjacent
324 to the skeletal remains. C1 = control from outside the grave cut, C2 = control from fill at the edge of
325 the grave above the level of the skeleton, C3 = control of the grave fill, level with the skeleton.

326 Branched chain fatty acids (*i*-$C_{15:0}$, *ai*-$C_{15:0}$, *i*-$C_{17:0}$, and *ai*-$C_{17:0}$) are significant components of bacterial
327 lipids while being scarce in other sources. The spatial variation of these components in the Anglo-
328 Scandinavian grave (Fig. 2c) was also mirrored by a series of C_{30}-C_{33} hopanoic acids and hopanols (e.g.
329 Fig. 2c), diagenetic products of the bacteriohopanetetrol and/or aminobacteriohopanetriol
330 components of bacterial cell membranes (Quirk et al., 1984; Winkler et al., 2001). The variability in
331 the bacterial markers across the remains (Fig. 2c) may be explained by the development and spread
332 of populations evolved from the gut microbial fauna during decomposition (Can et al., 2014) together
333 with soil microbe invasion in response to the corpse providing a plentiful supply of organic substrate.
334 Anatomical locations where the highest proportions of body tissue are distributed appear to contain
335 more abundant bacterial markers, indicating more intense/protracted microbial activity.

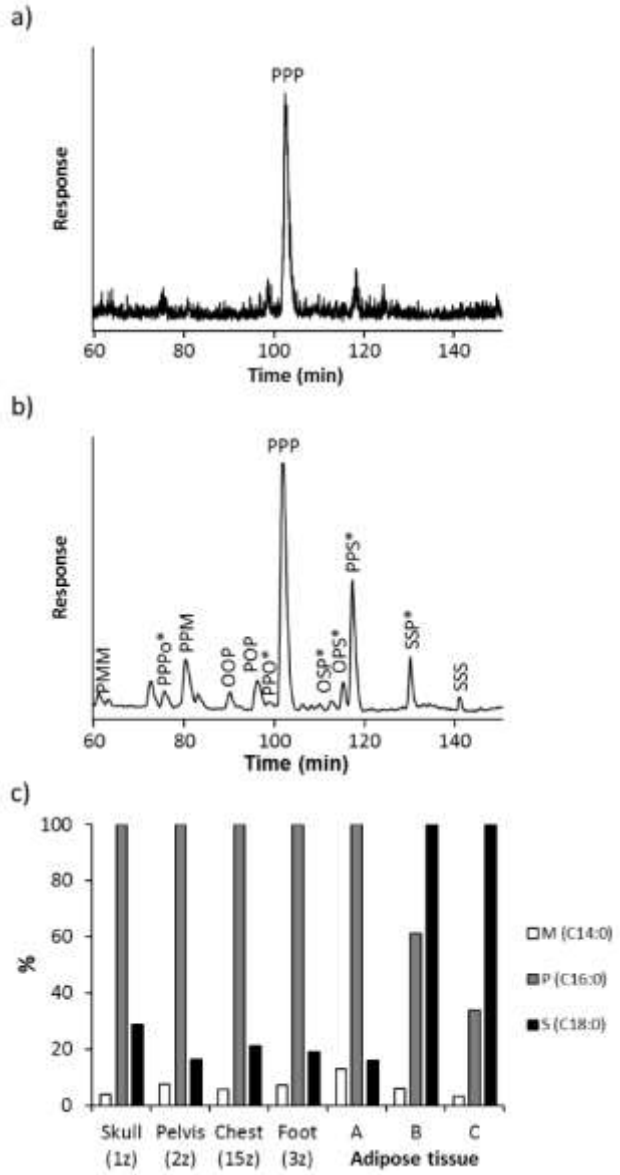

Figure 3. Partial HPLC-MS chromatograms (*m/z* 300-950) of the total lipid extracts for **a)** the control (C1) and **b)** pelvis (2) from C53700 acquired using Method J (Hasan, 2010). Triacylglycerols (TAGs) are labelled with letters to denote the acyl moieties attached to the glycerol backbone e.g. tripalmitin = PPP. M = myristyl ($C_{14:0}$), P = palmityl ($C_{16:0}$), Po = palmitoleyl ($C_{16:1}$), S = stearyl ($C_{18:0}$) and O = oleyl ($C_{18:1}$). *Indicates that only one of several possible positional isomers is shown. **c)** Comparison of the relative abundances of saturated TAG fatty acids (M = $C_{14:0}$, P = $C_{16:0}$ and S = $C_{18:0}$), normalised to the major component, in the soil samples from around the skeletal remains of C53700 to those of fresh human adipose tissue (Hodson et al., 2008). A = relative abundance of saturated fatty acids for human adipose tissue; B = relative abundance of saturated fatty acids for human adipose tissue assuming reduction of all monounsaturated fatty acids to saturated components; C = relative abundance of saturated fatty acids for human adipose tissue assuming reduction of all unsaturated fatty acids to saturated components.

In both graves the animal sterol cholest-5-en-3β-ol (cholesterol) was generally present in greater concentration in the samples associated with skeletal remains than in the controls (e.g. Fig. 4a) with the Anglo-Scandinavian burial having the higher concentrations. The preservation state of the Roman skeletal remains, C51364, was extremely poor compared with the Anglo-Scandinavian remains, consistent with its greater age and wetter burial environment. Interestingly, cholesterol concentrations were more varied, being particularly pronounced for soils associated with the more degenerated regions of the skeleton, closest to an Anglo-Scandinavian age cess pit that was proximal to the upper left hand side of the remains at a level slightly above the burial (Fig. 4a). Identification of cholesterol as a significant lipid component of archaeological bone (Evershed et al., 1995; Jim et al., 2004) together with the degenerated skeletal remains indicate it to have been released into the soil as the bone degraded. Hence, persistent cholesterol signatures may have value in aiding the identification of the original location of human remains in graves where the bones have not survived, subject to appropriate caution being exercised to differentiate signatures from alternative sources such as soil fauna. The cholesterol in the extracts was accompanied by its reduction products 5α-cholestan-3β-ol and 5β-cholestan-3β-ol (coprostanol). 5α-Cholestan-3β-ol is the major product of microbial reduction of cholesterol in soils and plant and mammalian tissues (Bethell et al., 1994). Its epimer, 5β-cholestan-3β-ol, typically a minor product of cholesterol reduction in the environment, is formed in significant amounts during microbial transformation of cholesterol in the guts of most higher animals and is the major sterol in human faecal material (Leeming et al., 1996). Accordingly, the ratio of 5β/(5α + 5β) cholestanols has been used as a proxy to indicate faecal contamination of sediments and water systems: values >0.7 indicate pollution (Grimalt et al., 1990). For the Anglo-Scandinavian grave, 5β/(5α + 5β) cholestanol index values suggestive of faecal contamination were restricted to the samples from the pelvic region, signifying inputs from the gastrointestinal tract. For the Roman grave, however, high ratios were observed throughout the burial (Fig. 4b), revealing clear evidence for the ingress from the cess pit of material having a strong faecal signature. The high 5β/(5α + 5β) cholestanol index values of samples from the cess pit combined with their lower cholesterol levels than the closest samples from within the grave fully support the interpretations discussed above. Despite the influence of the cess pit, the organic signature from the pelvic region of C51364 can still be distinguished by abundant bacterially-derived C_{30}-C_{33} hopanoic acids (Fig. 4c). Furthermore, hopanoic acid distributions at the feet suggest migration of gut-derived organic matter within the coffin. The evidence for organic signatures derived from the cess pit leachate affecting the preservation of the bones comes from the generally worse preservation of the skeletal remains nearer to the pit. Hence ingress of leachate from the Anglo-Scandinavian age cess pit into the grave contributed a strong faecal signature to the soils of the upper left section of the remains. Such organic

rich leachate would have been strongly anoxic and acidic, the latter accounting for the decalcification of the bone and consequent liberation of cholesterol within its area of influence. The acidic and reducing nature of the leachate means that it would have also carried ferrous iron in solution and is likely to have played a significant role in controlling phosphate levels in the Roman grave, mobilisation of phosphate being most prevalent in mildly acidic solutions (Nriagu, 1972). The absence/low levels of phosphorus in the burial soils of the Roman grave may be due either to low input to the original sediment or, given the greater age of the Roman burial, to the natural decrease in phosphorus levels with soil weathering (Cross and Schlesinger, 1995).

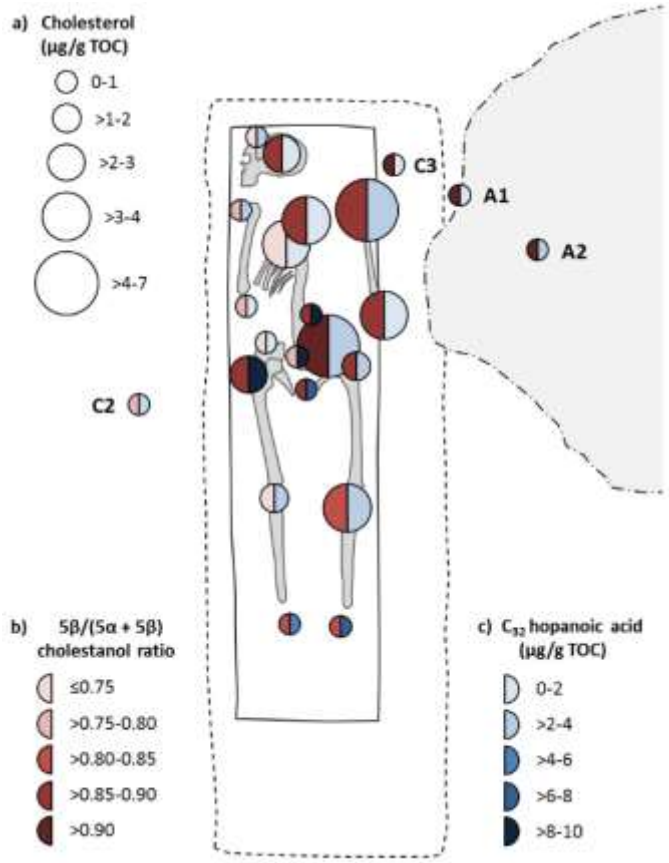

Figure 4. Variation in concentrations of specific lipids in Roman age burial C51364: **a)** cholesterol (circle sizes), **b)** 5β-cholestanol/(5α-cholestanol + 5β-cholestanol) ratio (red shades) and **c)** bishomohopanoic acid (C_{32}; blue shades). C2 = control from natural soil of grave cut above skeleton, C3 = control of grave fill level with top of skull, A1 = soil from natural soil of cess pit cut, A2 = soil excavated from the cess pit. The solid line outlines the soil stain from a coffin, the dashed line outlines the grave cut and the dashed and dotted line marks the boundary of an Anglo-Scandinavian age cess pit that cuts the grave.

Micromorphological analysis of undisturbed soil from control C3 and the head, pelvis and feet of the Roman burial revealed spherulites, features absent from control C2 and from all samples from the Anglo-Scandinavian burial. Morphological differences allowed the spherulites to be classified into

three distinct groups (Fig. 5, Table 2a). Group 1 spherulites: were mostly present near the skull and feet, and were less abundant near the pelvis. They occurred as infillings in the pores and within the fine material in the areas of the skull and pelvis with intermediate size range (Figs 5 and 6). Around the feet a smaller and narrower size range was present sealed between well preserved layered coatings of Fe rich fine material. Group 2 spherulites were present as infillings in pores and among mineral grains. They were most abundant in C3 and around the pelvis, with lower levels present in the skull area and only traces at the feet (Fig. 5). In some cases, the spherulites had coalesced to form dumbbell structures (Fig, 6a). Group 3 was identified only around the pelvis; some presented two distinct layers with high contrast at their junction with only the outer part of the spherule showing Maltese cross extinction and the core appearing amorphous in XPL.

Designation	Morphology and optical characteristics PPL XPL	Size / µm	Frequency / %	Location
Group 1	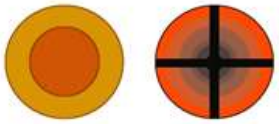	5-12	5-10	skull
			2-5	pelvis
		2-10	10-20	feet
Group 2	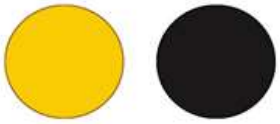	5-20	10-20	C3
			2-5	skull
			10-20	pelvis
			<2-5	feet
Group 3	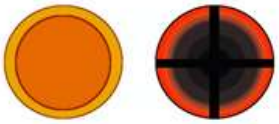	5-15	5-10	pelvis

Figure 5. Key characteristics and occurrences of different forms of siderite present in the Roman grave from Hungate, York. Detailed of the different spherulite characteristics are given in Table 2a.

Scanning electron microscopy-energy dispersive X-ray spectroscopy (SEM-EDS) analysis revealed the spherulites to have appreciable Fe contents. Taking account of literature reports (Driese et al., 2010; Ludvigson et al., 2013; Pye et al., 1990), the composition is attributed to siderite ($FeCO_3$). Pedogenic siderite is characteristic of wet and persistent saturated soils (Browne and Kingston, 1993), often in association with vivianite and more rarely with goethite, where it occurs as small crystallites or spherulitic aggregates in the groundmass or as pore infillings (Stoops and Delvigne, 1990). It forms as a colourless mineral in reducing conditions, remaining stable at neutral to basic pH and can only precipitate from weakly acid solution if the concentration of dissolved iron is abnormally high (Lemos

et al., 2007). Siderite spherules have been observed in organic-rich archaeological floor deposits, in areas inhabited by livestock where reducing conditions were inferred (Gebhardt and Langohr, 1999; Milek, 2012). The Fe contents of the Group 1 spherulites were greater than those of Group 2, with those of Group 1 from the area of the feet also having higher levels of Ca. Group 3 spherulites were characterized by an Fe rich corona with significantly lower Fe levels in the core. This difference is evident in the SEM-EDS images as a bright outer ring and a dull centre (Fig. 6d). The spherulites of the first group showed the highest reflectivity. Sideritic spherulites were observed in several other graves from Hungate, though exclusively in the sediments surrounding the skeletons and not in the upper layers of the backfill, occurring in association with vivianite. The Roman grave, C51364, was unique among those examined from Hungate in containing fan-like crystals of goethite and an absence of vivianite. The location of the goethite crystals within soil pores around the skull indicate it to be a secondary mineral (Fitzpatrick and Schwertmann, 1982) and the multi-layered fan-like coatings indicate that the soil was very wet (Stoops and Delvigne, 1990). Goethite is formed under changing redox conditions, being produced in intense oxidizing periods (Lindbo et al., 2010). Following oxidative weathering, siderite is converted to goethite, assuming brownish colours (Stoops and Delvigne, 1990).

The siderite in the Roman grave formed in the sediments surrounding the skeleton during a phase of reducing conditions, suggested to be associated with the decomposition of the organic matter of the corpse and the coffin under water-logged conditions. The higher frequency of siderite associated with the pelvis can be explained by the greater organic matter content and the consequently more intense reducing sub-environment. Furthermore, the amorphous nature of the cores of the Group 2 spherulites may reflect inhibition of crystallisation by the higher amounts of organic matter associated with the torso (cf. Fitzpatrick and Schwertmann, 1982). The orange colour of the siderite is indicative of partial oxidation, presumably resulting as the decay of organic matter slowed reducing oxygen sequestration and/or caused by the excavation, during Anglo-Scandinavian times, of the cesspit located in the proximity of the skull and pelvis and partially cutting the backfill (Fig. 4). The excavation of the cesspit most likely increased water flow through the grave, causing oxygenation. Further evidence for higher fluid flow comes from the amorphous phosphatic coatings around the pore walls in the C3 sample, located in the proximity of the cesspit. During the oxidative phase the sideritic spherules from the sediments closest to the cess pit (C3) underwent the most extensive weathering and goethite fan-like crystals were formed within C3 and on the pore walls in the area around the skull. The presence of the Fe-rich corona on the Group 3 spherulites indicates a period of intense anoxia during which the Fe-rich deposits accumulated, consistent with leaching and precipitation of Fe derived from the cess pit following its extended use. The higher Ca contents of the spherulites from the area of the feet can be attributed an origin from their proximity to bone and limited extent

of decalcification, the smaller size and higher Fe contents resulting from their rapid sealing and preservation by fine material coatings. Notably, the results from the analysis of the spherulites are entirely consistent with the interpretation from the profiles of the organic signatures and loss of bone from the area of the grave closest to the cess pit.

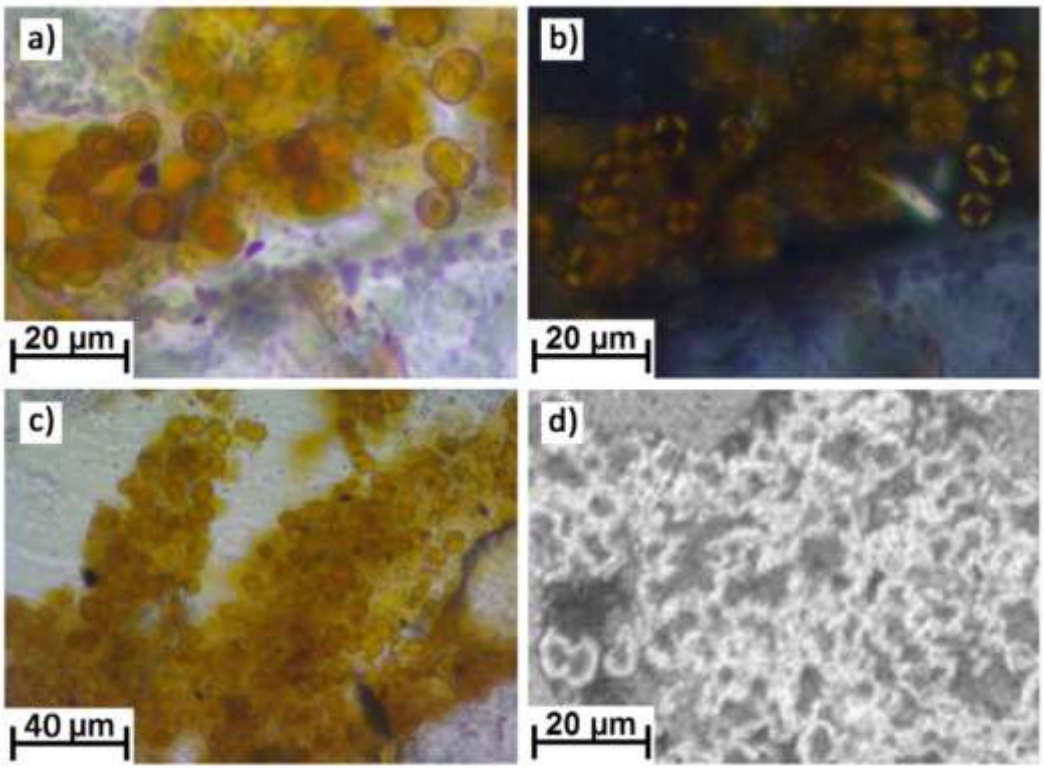

Figure 6. Sideritic spherulites in the Roman age burial C51364: a) and b) from the area of the skull, showing layered structure in PPL and characteristic Maltese cross extinction in XPL, c) accumulation in packing voids in the area of the pelvis and d) showing elemental compositional variation with Fe-rich outer rim in SEM-EDS image.

4 Conclusions

GC-MS and HPLC-MS^n analyses revealed distinct spatial variations in lipid profiles within the graves. TAGs, derived from adipose tissue, were observed in the extracts from both graves, being most abundant in samples from around the torso. The TAG acyl chain distributions, dominated by saturated components, suggest loss of unsaturated components, either by oxidative cleavage of the unsaturated bonds or by preferential hydrolysis of the unsaturated acyl moieties, rather than reductive transformation into saturated components. The highest levels of DAGs, MAGs, fatty acids and *n*-alkan-1-als also represent inputs from degraded body tissues and were observed in extracts from the upper torso and pelvis. *n*-Alkan-1-als, by virtue of their formation from reductive transformation of fatty acids and their survival in the soil, indicate regions of persistent anoxia within the grave. Their

preservation is highly localised to regions on the skeleton (e.g. skull, pelvis) where the bone morphology provides a barrier to free movement of water thus can allow anoxic conditions to develop. The higher abundances of microbial markers (branched chain fatty acids and hopanoids) in samples from around the skeleton than in the controls reflects a legacy of increased microbial activity in response to the remains, most likely through their involvement with the degradation of the corpse. In the case of the Roman burial, abundant hopanoids clearly distinguish the gut region of the remains, while their occurrence at the feet indicates migration of some material derived from the gut to the foot of the coffin. The gut region of the Anglo-Scandinavian burial is characterised by elevated levels of the faecal sterol, coprostanol. By contrast, coprostanol is present throughout the Roman grave and instead records the ingress of material from an Anglo-Scandinavian age cess pit adjacent to the burial. The acidic and anoxic nature of the leachate is indicated by the mobilisation of ferrous iron and the formation and persistence of Fe-rich sideritic spherulites. It is clear that leachate from the cess pit has affected the preservation of the skeletal remains, which is notably worse in areas closest to the pit. Decalcification of the bone by acidic fluids from the cess pit has led to release of bone-cholesterol into the soil in those regions, and depleted Ca contents recorded in spherulites from the skull and pelvis. The spherulites record several changes in the redox conditions within the Roman grave, from their initial formation, during a phase of intense reducing conditions associated with decomposition of the corpse, to a phase of partial oxidation as the decay progressed and oxygen demand decreased. This was followed by a second, more intensive phase of oxidation associated with the construction of the cess pit and increased water flow through the grave, indicated by goethite formation and phosphatic coatings on pore walls in the controls. An intense period of anoxia then followed with the extended usage of the cess pit, marked by deposition on the spherulites of iron rich layers.

The results exemplified by analysis of the two graves demonstrate that a valuable unexploited archive of information pertinent to the taphonomic interpretation of human burials is recorded in the burial matrix. The results demonstrate the preservation of signatures relating to the body tissues and gut contents which have the potential to inform archaeological investigation of diet (body tissues) and last meals (gut contents) both within particular communities and between different communities. Furthermore, the recognition that such organic signatures can and do survive should provide a stimulus to further research. Notably, the potential for survival of signatures from grave offerings provides scope for gaining further insights into their nature and use. Understanding of the factors that influence the survival/destruction of organic signatures in graves could also reveal characteristics that relate to particular styles of burial. The methods described here could also have potential in the identification of temporary or disinterred graves including in determining the anatomical orientation from the chemical signatures preserved in the soil, though further research is necessary.

Acknowledgements

The research forms part of the InterArChive project and received funding from the European Research Council under the European Community's Seventh Framework Programme (FP7/2007-2013) / ERC grant agreement n° 230193. We would like to express our sincere thanks to York Archaeological Trust for allowing us to collect samples. Karl Heaton is thanked for acquiring the GC-MS data.

References

Barfield, L., 1994. The Iceman reviewed. Antiquity 68, 10–26.

Bethell, P.H., Goad, L.J., Evershed, R.P., Ottaway, J., 1994. The study of molecular markers of human activity - the use of coprostanol in the soil as an indicator of human fecal material. J. Archaeol. Sci. 21, 619–632.

Brothwell, D.R., 1981. Digging up Bones: the Excavation, Treatment and Study of Human Skeletal Remains, 3rd ed. British Museum (Natural History) and Oxford University Press.

Browne, G.H., Kingston, D.M., 1993. Early diagenetic spherulitic siderites from Pennsylvanian palaeosols in the Boss Point Formation, Maritime Canada. Sedimentology 40, 467–474. https://doi.org/10.1111/j.1365-3091.1993.tb01346.x

Buckley, S.A., Evershed, R.P., 2001. Organic chemistry of embalming agents in Pharaonic and Graeco-Roman mummies. Nature 413, 837–841.

Bull, I.D., Berstan, R., Vass, A., Evershed, R.P., 2009. Identification of a disinterred grave by molecular and stable isotope analysis. Sci. Justice 49, 142–149. https://doi.org/10.1016/j.scijus.2009.01.016

Bullock, P., Fedoroff, N., Jongerius, A., Stoops, G., Tursina, T., 1985. Handbook for Soil Thin Section Description. Waine Research Wolverhampton.

Burns, A., Pickering, M.D., Green, K.A., Pinder, A.P., Gestsdóttir, H., Usai, M.-R., Brothwell, D.R., Keely, B.J., 2017. Micromorphological and chemical investigation of late-Viking age grave fills at Hofstaðir, Iceland. Geoderma 306, 183–194. https://doi.org/10.1016/j.geoderma.2017.06.021

Can, I., Javan, G.T., Pozhitkov, A.E., Noble, P.A., 2014. Distinctive thanatomicrobiome signatures found in the blood and internal organs of humans. J. Microbiol. Methods 106, 1–7. https://doi.org/10.1016/j.mimet.2014.07.026

Courty, M.A., Goldberg, P., Macphail, R.I., 1989. Soils and Micromorphology in Archaeology. Cambridge University Press Cambridge.

Cross, A.F., Schlesinger, W.H., 1995. A literature review and evaluation of the. Hedley fractionation:

538 Applications to the biogeochemical cycle of soil phosphorus in natural ecosystems. Geoderma
539 64, 197–214. https://doi.org/10.1016/0016-7061(94)00023-4

540 Driese, S.G., Ludvigson, G.A., Roberts, J.A., Fowle, D.A., Gonzalez, L.A., Smith, J.J., Vulava, V.M., McKay,
541 L.D., 2010. Micromorphology and Stable-Isotope Geochemistry of Historical Pedogenic Siderite
542 Formed in PAH-Contaminated Alluvial Clay Soils, Tennessee, U.S.A. J. Sediment. Res. 80, 943–
543 954. https://doi.org/10.2110/jsr.2010.087

544 Eglinton, G., Hamilton, R.J., 1967. Leaf epicuticular waxes. Science (80-.). 156, 1322–1335.
545 https://doi.org/10.1126/science.156.3780.1322

546 Eigenbrode, J.L., Freeman, K.H., Summons, R.E., 2008. Methylhopane biomarker hydrocarbons in
547 Hamersley Province sediments provide evidence for Neoarchean aerobiosis. Earth Planet. Sci.
548 Lett. 273, 323–331. https://doi.org/10.1016/j.epsl.2008.06.037

549 Evershed, R.P., 2008. Organic residue analysis in archaeology: the archaeological biomarker
550 revolution. Archaeometry 50, 895–924. https://doi.org/10.1111/j.1475-4754.2008.00446.x

551 Evershed, R.P., Connolly, R.C., 1988. Lipid preservation in Lindow man. Naturwissenschaften 75, 143–
552 145. https://doi.org/10.1007/bf00405306

553 Evershed, R.P., Turnerwalker, G., Hedges, R.E.M., Tuross, N., Leyden, A., 1995. Preliminary-results for
554 the analysis of lipids in ancient bone. J. Archaeol. Sci. 22, 277–290.

555 Fitzpatrick, E.A., 1993. Soil microscopy and micromorphology. John Wiley & Sons Ltd, West Sussex.

556 Fitzpatrick, R.W., Schwertmann, U., 1982. Al-Substituted goethite--an indicator of pedogenic and
557 other weathering environments in South Africa. Geoderma 27, 335–347.

558 Forbes, S.L., Stuart, B.H., Dent, B.B., 2002. The identification of adipocere in grave soils. Forensic Sci.
559 Int. 127, 225–230. https://doi.org/10.1016/S0379-0738(02)00127-5

560 Garnier, N., Rolando, C., Høtje, J.M., Tokarski, C., 2009. Analysis of archaeological triacylglycerols by
561 high resolution nanoESI, FT-ICR MS and IRMPD MS/MS: Application to 5th century BC-4th
562 century AD oil lamps from Olbia (Ukraine). Int. J. Mass Spectrom. 284, 47–56.
563 https://doi.org/10.1016/j.ijms.2009.03.003

564 Gebhardt, A., Langohr, R., 1999. Micromorphological Study of Construction Materials and Living Floors
565 in the Medieval Motte of Werken (West Flanders, Belgium). Geoarchaeology - An Int. J. 14, 595–
566 620. https://doi.org/10.1002/(SICI)1520-6548(199910)14:7<595::AID-GEA1>3.0.CO;2-Q

567 Ghislandi, S., 2016. Graves under the microscope: micromorphological study of sediments in
568 archaeological burials. University of York.

569 Gilbertson, J.R., Ferrell, W.J., Gelman, R.A., 1967. Isolation and analysis of free fatty aldehydes from
570 rat, dog ,and bovine heart muscle. J. Lipid Res. 8, 38–45.

571 Goldberg, P., Macphail, R.I., 2003. Short contribution: Strategies and techniques in collecting
572 micromorphology samples. Geoarchaeology 18, 571–578. https://doi.org/10.1002/gea.10079

573 Grimalt, J.O., Fernandez, P., Bayona, J.M., Albaiges, J., 1990. Assessment of fecal sterols and ketones
574 as indicators of urban sewage inputs to coastal waters. Environ. Sci. Technol. 24, 357–363.
575 https://doi.org/10.1021/es00073a011

576 Gulaçar, F.O., Susini, A., Klohn, M., 1990. Preservation and postmortem transformations of lipids in
577 samples from a 4000-year-old Nubian mummy. J. Archaeol. Sci. 17, 691–705.

578 Hadian, M., Good, I., Pollard, A.M., Zhang, X., Laursen, R., 2012. Textiles from Douzlakh Salt Mine at
579 Chehr Abad, Iran: a technical and contextual study of Late pre-Islamic Iranian textiles. Int. J.
580 Humanit. Islam. Repub. Iran 19, 152–173.

581 Hasan, H., 2010. Development of an LC-MS/MS Method for the Analysis of Triacylglycerols from Meat
582 and Application in the Discrimination of Cooked Meat Products. Ph.D. Thesis, Univ. York. PhD
583 thesis, University of York UK.

584 Hita, C., Parlanti, E., Jambu, P., Joffre, J., Amblès, A., 1996. Triglyceride degradation in soil. Org.
585 Geochem. 25, 19–28. https://doi.org/10.1016/S0146-6380(96)00107-6

586 Hodson, L., Skeaff, C.M., Fielding, B.A., 2008. Fatty acid composition of adipose tissue and blood in
587 humans and its use as a biomarker of dietary intake. Prog. Lipid Res. 47, 348–380.
588 https://doi.org/10.1016/j.plipres.2008.03.003

589 Jensen, R.G., Dejong, F.A., Lambertdavis, L.G., Hamosh, M., 1994. Fatty-acid and positional selectivities
590 of gastric lipase from premature human infants - in-vitro studies. Lipids 29, 433–435.
591 https://doi.org/10.1007/bf02537313

592 Jim, S., Ambrose, S.H., Evershed, R.P., 2004. Stable carbon isotopic evidence for differences in the
593 dietary origin of bone cholesterol, collagen and apatite: implications for their use in
594 palaeodietary reconstruction. Geochim. Cosmochim. Acta 68, 61–72.
595 https://doi.org/10.1016/s0016-7037(03)00216-3

596 Kimpe, K., Jacobs, P.A., Waelkens, M., 2001. Analysis of oil used in late Roman oil lamps with different
597 mass spectrometric techniques revealed the presence of predominantly olive oil together with
598 traces of animal fat. J. Chromatogr. A 937, 87–95. https://doi.org/10.1016/S0021-
599 9673(01)01304-8

Leeming, R., Ball, A., Ashbolt, N., Nichols, P., 1996. Using faecal sterols from humans and animals to distinguish faecal pollution in receiving waters. Water Res. 30, 2893–2900.

Lemos, V.P., Da Costa, M.L., Lemos, R.L., De Faria, M.S.G., 2007. Vivianite and siderite in lateritic iron crust: An example of bioreduction. Quim. Nova 30, 36–40. https://doi.org/10.1590/S0100-40422007000100008

Lindbo, D.L., Stolts, M.H., Vepraskas, M.L., 2010. Redoximorphic Features, in: Stoops, G., Marcelino, V., Mees, F. (Eds.), Interpretation of Micromorphological Features of Soils and Regoliths. Elsevier, UK.

Ludvigson, G.A., González, L.A., Fowle, D.A., Roberts, J.A., Driese, S.G., Villarreal, M.A., Smith, J.J., Suarez, M.B., 2013. Paleoclimatic Applications and Modern Process Studies of Pedogenic Siderite. New Front. Paleopedol. Terr. Paleoclimatology 79–87. https://doi.org/10.2110/sepmsp.104.01

Mayer, B.X., Reiter, C., Bereuter, T.L., 1997. Investigation of the triacylglycerol composition of Iceman's mummified tissue by high-temperature gas chromatography. J. Chromatogr. B 692, 1–6.

Miedema, R., Pape, T., Van der Waal, G.J., 1974. A method to impregnate wet soil samples, producing high-quality thin sections. Netherlands J. Agric. Sci. 22, 37–39.

Milek, K.B., 2012. Floor formation processes and the interpretation of site activity areas: An ethnoarchaeological study of turf buildings at Thverá, northeast Iceland. J. Anthropol. Archaeol. 31, 119–137.

Mirabaud, S., Rolando, C., Regert, M., 2007. Molecular criteria for discriminating adipose fat and milk from different species by nanoESI MS and MS/MS of their triacylglycerols: Application to archaeological remains. Anal. Chem. 79, 6182–6192. https://doi.org/10.1021/ac070594p

Nriagu, J., 1972. Stability of vivianite and ion-pair formation in the system $Fe_3(PO_4)_2$-$H_3PO_4H_3PO_4$-H_2O. Geochim. Cosmochim. Acta 36, 459–470.

O'Connor, S., Ali, E., Al-Sabah, S., Anwar, D., Bergström, E., Brown, K.A., Buckberry, J., Buckley, S., Collins, M., Denton, J., Dorling, K.M., Dowle, A., Duffey, P., Edwards, H.G.M., Faria, E.C., Gardner, P., Gledhill, A., Heaton, K., Heron, C., Janaway, R., Keely, B.J., King, D., Masinton, A., Penkman, K., Petzold, A., Pickering, M.D., Rumsby, M., Schutkowski, H., Shackleton, K.A., Thomas, J., Thomas-Oates, J., Usai, M.-R., Wilson, A.S., O'Connor, T., 2011. Exceptional preservation of a prehistoric human brain from Heslington, Yorkshire, UK. J. Archaeol. Sci. 38, 1641–1654. https://doi.org/10.1016/j.jas.2011.02.030

632 Pickering, M.D., Lang, C., Usai, M.-R., Keely, B.J., Brothwell, D.R., 2014. Organic residue analysis of
633 soils, in: Loe, L., Boyle, A., Webb, H., Score, D. (Eds.), “Given to the Ground”: A Viking Age Mass
634 Grave on Ridgeway Hill, Weymouth. Dorset Natural History and Archaeological Society
635 Monograph Series Vol 23, Oxbow Books Oxford, pp. 237–245.

636 Pye, K., Dickson, J.A.D., Schiavon, N., Coleman, M.L., Cox, M., 1990. Formation of Siderite - Mg-Calcite
637 - Iron Sulfide Concretions in Intertidal Marsh and Sandflat Sediments, North-Norfolk, England.
638 Sedimentology 325–343.

639 Quirk, M.M., Wardroper, A.M.K., Wheatley, R.E., Maxwell, J.R., 1984. Extended hopanoids in peat
640 environments. Chem. Geol. 42, 25–43. https://doi.org/10.1016/0009-2541(84)90003-2

641 Raclot, T., Groscolas, R., 1993. Differential mobilization of white adipose-tissue fatty-acids according
642 to chain-length, unsaturation, and positional isomerism. J. Lipid Res. 34, 1515–1526.

643 Rapport, M.M., Lerner, B., 1959. The structure of plasmalogens IV. Lipids in normal and neoplastic
644 tissues of man and in normal tissues of rabbit and rat. Biochim. Biophys. Acta 33, 319–325.
645 https://doi.org/10.1016/0006-3002(59)90119-2

646 Šoberl, L., Gasparic, A.Z., Budja, M., Evershed, R.P., 2008. Early herding practices revealed through
647 organic residue analysis of pottery from the early Neolithic rock shelter of Mala Triglavca ,
648 Slovenia. Doc. Praehist. 15, 253–260. https://doi.org/10.4312/dp.35.19

649 Stead, I.M., Bourke, J.B., Brothwell, D.R., 1986. Lindow Man: The Body in the Bog. British Museum
650 Publications, London.

651 Stoops, G., 2003. Guidelines for Analysis and Description of Soil and Regolith Thin-Sections. Soil
652 Science Society of America Madison.

653 Stoops, G., Delvigne, J., 1990. Morphology of Mineral Weathering and Neoformation. II
654 Neoformations. Dev. Soil Sci. 19, 483–492.

655 Stott, A.W., Evershed, R.P., Jim, S., Jones, V., Rogers, J.M., Tuross, N., Ambrose, S., 1999. Cholesterol
656 as a new source of palaeodietary information: experimental approaches and archaeological
657 applications. J. Archaeol. Sci. 26, 705–716. https://doi.org/10.1006/jasc.1998.0386

658 Winkler, A., Haumaier, L., Zech, W., 2001. Variation in hopanoid composition and abundance in forest
659 soils during litter decomposition and humification. Org. Geochem. 32, 1375–1385.
660 https://doi.org/10.1016/s0146-6380(01)00115-2

661 Wittenberg, J.B., Korey, S.R., Swenson, F.H., 1956. Determination of higher fatty aldehydes in tissues.
662 J. Biol. Chem. 219, 39–47.

663